Robust Tuning of Grid-Forming Converters Using Kharitonov Theorem

Sharara Rehimi[1], Hassan Bevrani[2], Chiyori Urabe[1], Takeyoshi Kato[1] and Toshiji Kato[3]
[1]*Electrical Engineering Department, Institute of Materials and Systems for Sustainability, Nagoya University, Tsurumaicho Str. 65, Showa Ward, Nagoya, Japan*
[2]*Electrical Engineering Department, Smart/Micro Grids Research Center, University of Kurdistan, Pasdaran Boulevard, PO Box 416, Sanandaj, Iran*
[3]*Electrical Engineering Department, Doshisha University, Gembucho Str. 601, Kamigyo-ku, Kyoto, Japan*
rehimi.sharara.z8@s.mail.nagoya-u.ac.jp, bevrani@uok.ac.ir, urabe.chiyori.c0@f.mail.nagoya-u.ac.jp, kato.takeyoshi.b5@f.mail.nagoya-u.ac.jp, tkato@mail.doshisha.ac.jp

Keywords: Kharitonov Theorem, Grid-Forming Converters, Robust Tuning, Modern Power Grids.

Abstract: This paper presents a study on the robust tuning of damping coefficient, inertia, and conventional controller gains for a grid-forming converter connected to the main grid. The proposed method is evaluated using the Typhoon Hill system, which allows for comprehensive simulation and analysis. The Kharitonov theorem is utilized to achieve robustness in the face of deviations in line parameters. Unlike previous works, our approach systematically and graphically searches for a non-conservative Kharitonov region in the solution area of the controller coefficients. This region characterizes all stabilizing gain controllers that effectively stabilize an uncertain control structure. By selecting coefficients from the obtained non-conservative Kharitonov region, the synthesized controller effectively stabilizes the grid-forming converter. The results of this study highlight the efficacy of the Kharitonov theorem in achieving robust tuning of essential parameters for grid-forming converters, enhancing stability and performance in the presence of line parameter variations.

1 INTRODUCTION

1.1 Modern Power Grids

In recent years, there has been a notable increase in the integration of renewable energy sources (RESs) into the modern power grids, driven by the demand for sustainable and environmentally friendly energy solutions. Power electronic interface converters (grid connected converters) are essential for connecting RESs to the grid, enhancing controllability and enabling RESs to contribute effectively to grid objectives. Researchers have focused on improving the efficiency of these converters, leading to significant advancements in power converter technology [1].

Grid connected converters can be categorized as grid forming converters (GFM) and grid following converters (GFL). The GFM converters, acting as voltage sources, offer greater flexibility compared to GFL converters, which function as current sources. Various control methods have been developed to fully utilize the capabilities of GFM converters. In addition to connecting RESs to the grid, GFM converters can provide ancillary services such as frequency adjustment, voltage regulation, improved inertial response, damping enhancement, and power factor correction [2].

The significance of GFM converters lies in their ability to meet the diverse needs of modern power grids. Power companies, particularly those heavily reliant on RESs, are revising their grid codes to leverage the capabilities of GFM converters and optimize their support to the main grid. This strategic response allows for enhanced integration of RESs and maximizes grid interaction, positioning GFM converters as integral interfaces in the modern power systems [2].

Robust tuning of control coefficient in the control system of a GFM is a crucial aspect of ensuring stable and reliable operation in modern power grids. The GFMs play a vital role in maintaining grid stability and providing ancillary services. However, uncertainties in line parameters and operating conditions can affect the performance of the converter control system. To address this challenge, researchers

have focused on robust tuning of control coefficients in the control system of the GFMs [3].

1.2 Robust Control Approach

Robust tuning involves selecting appropriate values for the most important control gains in the GFM control system to ensure system stability and resilience in the face of parameter variations. The Kharitonov theorem has emerged as a powerful tool in this context [4]. It allows for a systematic and graphical search for a non-conservative Kharitonov region in the controller coefficient parameter space. This region represents all stabilizing Proportional-Integral-Derivative (PID) controllers that can effectively stabilize an uncertain control system. By selecting coefficients from this region, the synthesized controller can effectively stabilize the GFM.

As mentioned, the Kharitonov theorem is a key tool used in several studies to design robust controllers for uncertain control systems. A study in [5] provides an elementary proof of the Kharitonov theorem based on Bezoutian matrices. This proof establishes a unified derivation of Kharitonov-like theorems for both continuous-time and discrete-time settings. The study introduces the concept of (block) Anderson-Jury Bezoutians and suggests a potential technique to address a robust stability problem in the multi input-multi output (MIMO) case. In [6], the theorem is applied to synthesize stabilizing controllers for interval plants. The study focuses on designing a controller that can stabilize multiple Kharitonov-defined vortex polynomials simultaneously. Through the search of a non-conservative Kharitonov region, the controller is systematically developed within the bounds of all stabilizing PID controllers for uncertain plants. The study also incorporates a virtual gain phase margin tester compensator to ensure robust safety margins.

Authors in [7] propose a tuning strategy for robust static output feedback (SOF) controllers using Kharitonov's theorem. The goal is to minimize the quadratic cost of the controllers while considering multiple parametric uncertainties. The study utilizes Kharitonov's theorem to define a family of bounded, robustly stable SOF controllers. An evolutionary algorithm is then employed to select the controller that minimizes the quadratic cost within this family. This approach addresses the computational complexity of the control problem's non-convex nature. In [8], a robust decentralized proportional-integral (PI) control design for load frequency control (LFC) in a multi-area power system is presented. The study optimizes the system's robustness margin and transient performance simultaneously by determining the PI controller parameters using Kharitonov's theorem. The theorem helps establish the maximal uncertainty bounds for stable power system performance, enabling the optimization of control objectives through techniques like genetic algorithms.

In the field of LFC, another study focuses on efficient control algorithms [9]. The paper explores the robustness of control algorithms based on fractional order control and interval modeling of the plant. By utilizing Kharitonov's theorem, a fractional order PID controller is designed for the interval model of a single area LFC. This approach allows engineers to define parameter limits that ensure satisfactory controller performance, leading to improved system stability and safety. Furthermore, these studies demonstrate the versatility and usefulness of the Kharitonov theorem in various control design applications, ranging from interval plants to power systems. The theorem enables the synthesis of stabilizing controllers, optimization of control objectives, and robustness analysis of control algorithms.

Meanwhile, authors in [10] present a method for designing robust power system stabilizers (PSSs). The stabilizing PSSs are characterized using d-decomposition, which divides the controller-parameter space into root-invariant regions. The designed control is applied to a single machine-infinite bus system (SMIB). The approach considers d-stability, which incorporates a pre-specified damping cone in the complex s-plane to improve time-domain specifications. The pole clustering in the damping cone is achieved by ensuring the Hurwitz stability of a complex polynomial. The parametric uncertainties caused by variations in load patterns are captured using an interval polynomial. The computation of the set of robust d-stabilizing PSSs requires checking the Hurwitz stability of a complex interval polynomial, which is addressed using a complex version of Kharitonov's theorem.

Besides, a study in [11], focuses on LFC of a microgrid in the presence of cyber-attacks. The paper proposes the application of the Kharitonov theorem-based proportional-integral (KT-PI) control technique. The microgrid consists of RESs, controllable energy sources, and energy storage systems. A denial-of-service (DoS) attack is considered as the cyber-attack scenario. The robustness and effectiveness of the KT-PI control technique are evaluated by considering parametric uncertainties and nonlinearities such as generation

rate constraint (GRC) and governor dead-band (GDB). Performance indices such as integral square error (ISE), integral absolute error (IAE), and integral of time absolute error (ITAE) are used for quantitative comparative analysis against the ZN-PI controllers. Then, the stability of the microgrid under the DoS attack is analyzed using the eigenvalue approach.

Another work addresses the robust stability analysis of an islanded microgrid with droop-controlled inverter-based distributed generators (DGs) [12]. The low-frequency (LF) dominant modes of the microgrid can become unstable or highly oscillatory due to large load changes, microgrid structure reconfiguration, and higher-power demands. To address this, a robust two-degree-of-freedom (2DOF) decentralised droop controller is proposed for each DG unit. A new design procedure is presented to robustly determine the transient droop gains, which effectively damp the LF oscillatory modes of the microgrid in the presence of disturbances, equilibrium point variations, and uncertain parameters. Inspired by Kharitonov's stability theorem, a robust D-stability analysis is performed to determine the specific ranges of the transient droop gains.

Furthermore, another study is focused on the stability analysis of the pitch system control of a horizontal axis wind turbine using the Kharitonov robust stability method. The objective is to assess the robust stability of the pitch controller under uncertainties arising from varying operating conditions. The study utilizes the National Renewable Energies Laboratory (NREL) 5 MW class IIA wind turbine model. The proposed method demonstrates satisfactory response to limited variations in the models characteristics [13].

Additionally, a reduction method for higher-order interval systems based on Kharitonov's theorem is presented in [14]. The method utilizes differentiation to achieve a reduced-order interval model. It is applicable to both single-input single-output (SISO) and MIMO interval systems. The proposed method is mathematically simple and preserves the dominant characteristics of the original system in its reduced-order interval models. Stable reduced-order models are obtained if the original system is stable. The effectiveness of the technique is demonstrated through benchmark problems, showing close approximation to the original system. The proposed method is compared with other well-known reduction methods in terms of time response specifications and performance indices, validating its effectiveness and efficiency. Additionally, the method is extended for discrete-time interval systems.

The present study focuses on the extensive and impactful utilization of Kharitonovs theorem for robust coefficient adjustment of a GFM control systems. Specifically, the study applies this method to adjust the coefficients of the key parameters in the control system of GFM.

This paper is organized as follows: Section 2 presents the dynamic modeling of the case study. Section 3 describes the mathematical model used for performance evaluation of the proposed robust control method. In Section 4, the control design procedure based on Kharitonovs theorem is presented. Section 5 presents the simulation results, demonstrating the effectiveness of the proposed control strategy. Finally, Section 6 concludes the paper by summarizing the key findings and contributions of this study.

2 DYNAMIC MODELING

The GFM under investigation is connected with an LCL filter. Subsequently, the system is linked to the line impedance and then connected to the main power grid as shown in Figure 1. Here, the L_{f1}, R_{f1}, C_f, R_c, L_{f2}, R_{f2}, L_l, R_l and V_{DC} represent the filter inductor (left side), filter inductor ohmic resistance (left side), filter capacitor, filter capacitor ohmic resistance, filter inductor (right side), filter inductor ohmic resistance (right side), line inductor, line ohmic resistance, and DC voltage link, respectively. Furthermore, the control system is implemented on the GFM converter using pulse width modulation (PWM). Additional information regarding the control system unit is illustrated in Figure 2.

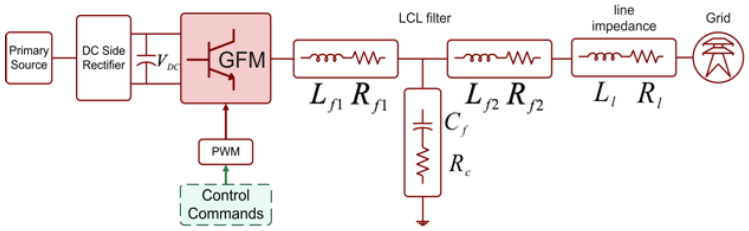

Figure 1: Grid connected converter structure: grid forming mode.

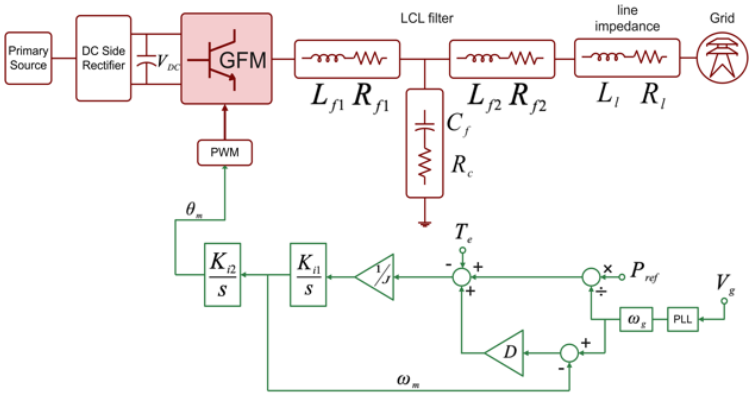

Figure 2: Active power control system of a grid forming converter.

.

The control system utilized in this paper includes active power control, as illustrated in Figure 2. Here, T_e, PLL, ω_g, P_{ref}, ω_m, J, K_{i1}, K_{i2}, D, V_g, and θ_m are electrical torque, phase-locked loop (PLL) dynamic (in this study considered 1), grid frequency, reference active power, measured frequency, inertia coefficient, first conventional control gain, second conventional control gain, damping coefficient, grid voltage and measured angle to be applied to the PWM, respectively.

3 MATHEMATIC MODEL

This section presents the mathematical model of the studied system, specifically focusing on the power section (LCL filter and line section) as shown in Figure 1. The main objective is to derive the transfer function (1) that maps the input voltage to the corresponding output voltage [1].

$$G_p = G_{Filter} G_{Line} . \quad (1)$$

Where G_p, G_{Filter}, and G_{Line} are the power section, LCL filter, and line transfer function, respectively. G_p can be calculated (2) as follows:

$$G_p = \frac{(A)s^6 + (B)s^5 + (C)s^4 + (H)s^3 + (F)s^2 - (E)s - (1)D}{(K)s^5 + (L)s^4 + (O)S^3 + (N)S^2 + (M)s} . \quad (2)$$

Once the transfer function of the power section in the studied system is obtained, the characteristic equation can be derived based on the obtained transfer function (3):

$$\Delta(s) = 1 + G_{Filter} G_{Line} K(s) = 0 , \quad (3)$$

where:

$$K_s = \frac{(Y)s}{(Z)s^2 + (R)s} , \quad (4)$$

and

$$\Delta(s) = a_6 s^6 + a_5 s^5 + a_4 s^4 + a_3 s^3 + a_2 s^2 + a_1 s^1 + a_0 - D . \quad (5)$$

The detailed parameters are available in the appendix section. Additionally, system parameters are given in Table 1.

Table 1: System parameters.

Parameter	Value	Parameter	Value
T_{fP}	0.0159 s	L_f	0.15pu
T_{fQ}	0.0157 s	R_f	0.005pu
ω_0	377 rad/s	L_l	0.15 pu
L_v	0.32pu	C_f	0.064 pu
R_v	0.03 pu	R_c	0.002 pu
S_{base}	5 kVA	v_0	200 V

4 PROBLEM STATEMENT

Optimizing the conventional controller gains within the control unit of a GFM is a challengeable task while considering uncertain conditions encountered in practical sites. KT offers a solution for assessing the stability of systems that possess uncertain parameters. The theorem is employed by examining the extreme scenarios of coefficient ranges to determine if the system remains stable across all possible coefficient values. In this study, KT is applied to optimize the parameters of GFM control unit under the uncertainties condition. To achieve this, the important control gains are computed based on the calculation of the Kharitonov polynomials. The controller parameters are selected from a specific region that exhibits the best behavior in the root locus plan.

5 CONTROL DESIGN PROCEDURE

The mathematical model of the system under consideration, which incorporates parametric uncertainties, is represented as follows (6):

$$\Delta(s) = [a_6^+, a_6^-]s^6 + [a_5^+, a_5^-]s^5 + [a_4^+, a_4^-]s^4 + [a_3^+, a_3^-]s^3 + [a_2^+, a_2^-]s^2 + [a_1^+, a_1^-]s^1 + [a_0^+, a_0^-] - D \quad (6)$$

Where a_i^+ and a_i are the lower and upper bounds of a_i, respectively. The polynomials for KT can be written as:

$$K1 = a_0^- + a_1^- s + a_2^+ s^2 + a_3^+ s^3 + a_4^- s^4 + a_5^- s^5 + a_6^+ s^6,$$
$$K2 = a_0^+ + a_1^+ s + a_2^- s^2 + a_3^- s^3 + a_4^+ s^4 + a_5^+ s^5 + a_6^- s^6,$$
$$K3 = a_0^- + a_1^+ s + a_2^+ s^2 + a_3^- s^3 + a_4^- s^4 + a_5^+ s^5 + a_6^+ s^6,$$
$$K4 = a_0^+ + a_1^- s + a_2^- s^2 + a_3^+ s^3 + a_4^+ s^4 + a_5^- s^5 + a_6^- s^6.$$

Considering 20% variation in the line parameters $(R_l - L_l)$, a_i^+ and a_i can be obtained and the polynomials for KT can be calculated. This study focuses on the adjustment of the inertia coefficient, damping coefficient, and conventional controller coefficient through robust-based techniques. By considering positive values for the inertia and damping coefficients, the admissible range of values for the target coefficients is determined to ensure stability for all Kharitonov polynomials. The stability regions corresponding to each polynomial are shown in Figure 3. The intersection of these regions represents the feasible solution area according to KT. The common solution area is illustrated in Figure 4. The basic geometry associated with the zero-exclusion condition, for $0 < \omega < 50$ kHz, is fully demonstrated in Figure 5. Based on the zero-exclusion condition closed-loop system with designed controller is robustly stable if and only if, the rectangle plots do not include the origin of plane. This issue is clearly confirmed in Figure 5.

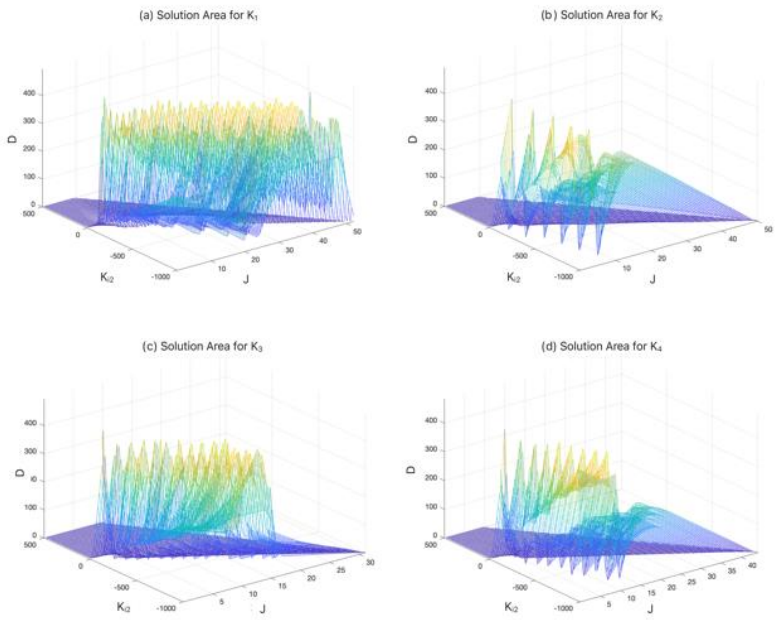

Figure 3: Stability regions corresponding to each polynomial: a) first KT polynomial, b) second KT polynomial, c) third KT polynomial, d) fourth KT polynomial.

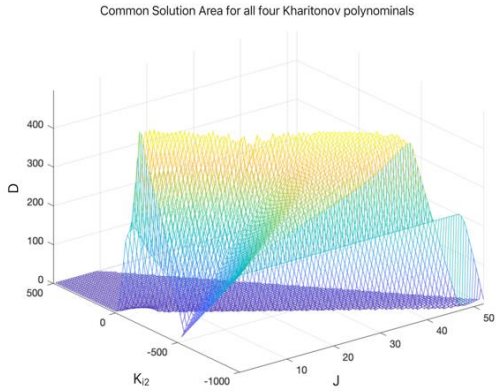

Figure 4: The common solution area for all four KT polynomials.

6 SIMULATION RESULTS

This section focuses on the evaluation of the controller gain values robustly tuned for active power control in a GFC control system. The Typhoon Hill software is employed to simulate and assess the effects of these proposed controller gains on the system. Figure 6 presents the configuration of the system under investigation within the Typhoon HIL software. Result illustrated in Figure 7, the system performance under normal conditions Figure 7a is depicted as being stable and acceptable. However, when a 20% variation is applied to the impedance values of the interconnecting line between the filter and the grid, the output power experiences fluctuations Figure 7b. By employing the proposed method to adjust the existing controller gains, the system behavior is restored to its normal state, thus achieving stability Figure 8c.

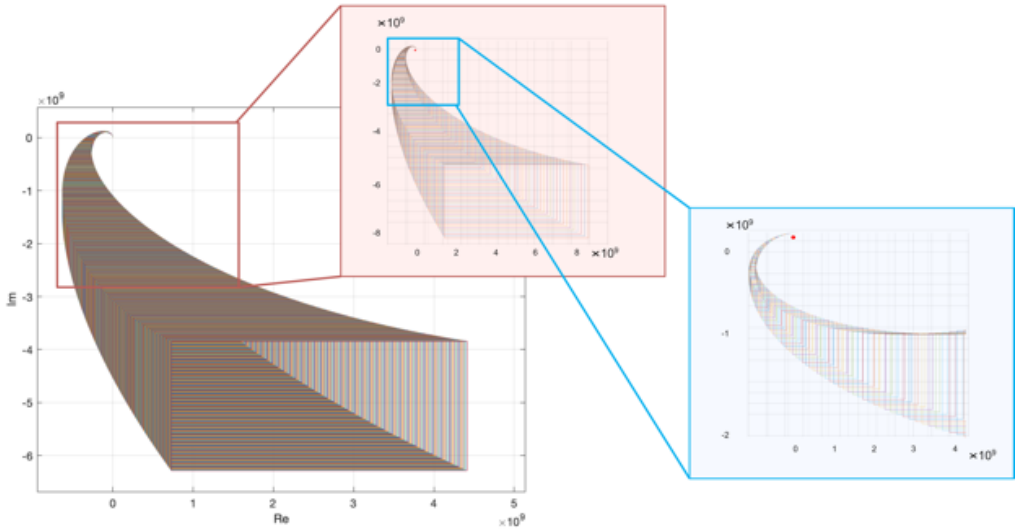

Figure 5: Motion of the Kharitonov's rectangle for 0 < ω< 50 kHz.

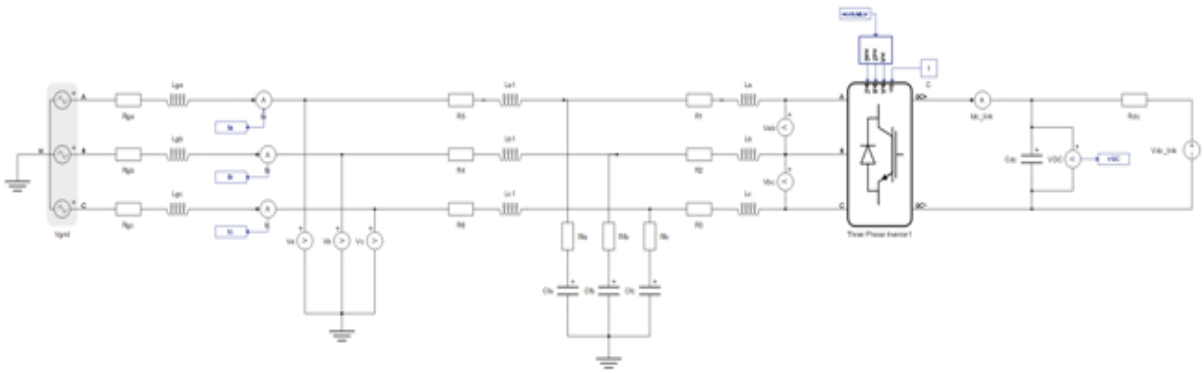

Figure 6: Grid forming converter: Typhoon HIL structure.

.

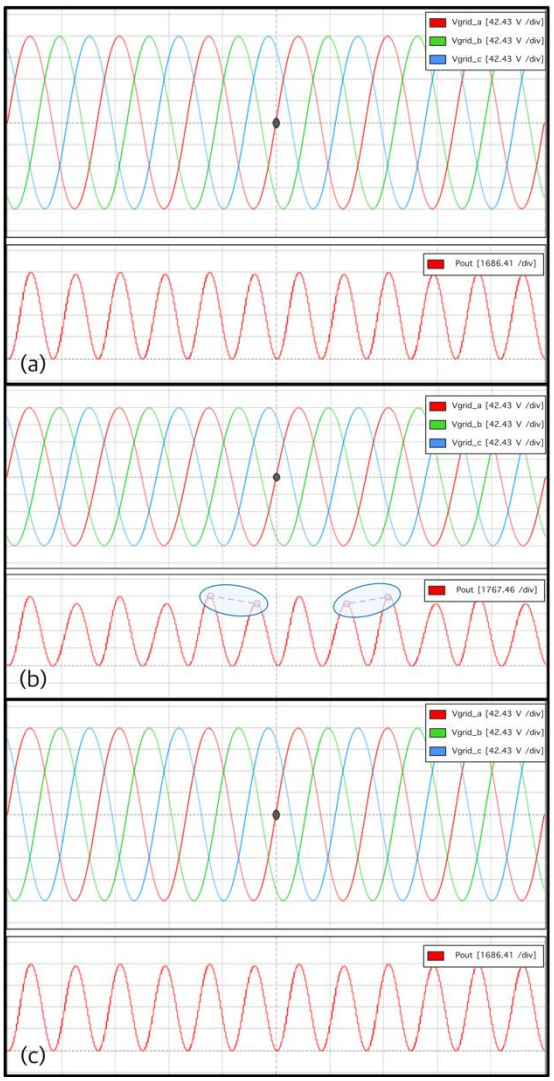

Figure 7: Voltage and active power: a) normal condition, b) 20% deviations in the line parameters with normal controller, c) 20% deviations in the line parameters with robust tuned controller.

7 CONCLUSIONS

This research employs Kharitonovs theory to determine the acceptable performance range of a grid-forming converter under conditions of uncertainty in the transmission lines parameters. By utilizing this methodology, the need for additional controllers to maintain system stability in the presence of uncertainty is eliminated. Instead, the existing conventional controllers can be re-tuned using this theory to effectively address situations involving uncertainty.

Indeed, this study demonstrates the effectiveness of the robust tuning of damping coefficient, inertia, and conventional controller gains in a grid-forming converters. By Using the Kharitonov theorem and utilizing the Typhoon Hill device for evaluation, the stability and enhanced performance in the presence of line parameter variations have successfully achieved. Through systematic and graphical exploration of the non-conservative Kharitonov region, authors have identified stabilizing existing controllers that effectively stabilize uncertain control structures. The findings of this study contribute to the field by providing a comprehensive approach to robust parameter tuning, ultimately strengthening the stability and reliability of grid-forming converters in practical applications.

ACKNOWLEDGMENTS

The authors acknowledge the financial support of KDDI Foundation, Japan. Also received support from Smart/Micro Grids Research Center (SMGRC) at the University of Kurdistan, Sanandaj, Iran is highly appropriated.

REFERENCES

[1] F. Blaabjerg, Y. Yang, K. A. Kim, and J. Rodriguez, "Power electronics technology for large-scale renewable energy generation," Proceedings of the IEEE, vol. 111, no. 4, pp. 335-355, Mar. 2023.

[2] H. Bevrani et al., "Grid Connected Converters, Modeling, Stability and Control," Elsevier, Radarweg 29, PO Box 211, 1000 AE Amsterdam, Netherlands, 2022.

[3] H. Bevrani, "Robust Power System Frequency Control," 2nd ed., J. H. Chow, A. M. Stankovic, and D. Hill, Eds. Springer, Cham Heidelberg New York Dordrecht London, 2014.

[4] B. R. Barmish, "New Tools for Robustness of Linear Systems," Macmillan Coll Div, 1993.

[5] A. Olshevsky and V. Olshevsky, "Kharitonov's Theorem and Bezoutians," Linear Algebra and its Applications, vol. 399, pp. 285-297, 2005.

[6] D. G. Padhan and S. Majhi, "Enhanced cascade control for a class of integrating processes with time delay," ISA Trans, vol. 52, no. 1, pp. 45-55, 2013.

[7] R. Toscano and P. Lyonnet, "Robust static output feedback controller synthesis using Kharitonov's theorem and evolutionary algorithms," Information Sciences, vol. 180, no. 10, pp. 2023-2028, 2010.

[8] M. R. Toulabi, M. Shiroei, and A. M. Ranjbar, "Robust analysis and design of power system load frequency control using the Kharitonov's theorem," International Journal of Electrical Power & Energy Systems, vol. 55, pp. 51-58, 2014.

[9] S. Sondhi and Y. V. Hote, "Fractional order PID controller for perturbed load frequency control using Kharitonov's theorem," International Journal of Electrical Power & Energy Systems, vol. 78, pp. 884-896, 2016.

[10] M. Ayman and M. Soliman, "Robust multi-objective PSSs design via complex Kharitonov's theorem," European Journal of Control, vol. 58, pp. 131-142, 2021.

[11] K. Sharma, A. K. Yadav, and B. B. Sharma, "Kharitonov theorem-based robust control approach for sustainable microgrid against DoS cyber-attack," Digital Chemical Engineering, 2023, 7.

[12] N. M. Dehkordi, N. Sadati, and M. Hamzeh, "Robust tuning of transient droop gains based on Kharitonov's stability theorem in droop-controlled microgrids," IET Generation, Transmission & Distribution, vol. 12, no. 14, pp. 3495-3501, 2018.

[13] N. Ravikumar and G. Saraswathi, "Robust Controller Design for Speed Regulation of a Wind Turbine using 16-Plant Theorem Approach," EAI Endorsed Transactions on Energy Web, vol. 6, no. 24, 2019.

[14] S. R. Potturu and R. Prasad, "Model Order Reduction of LTI Interval Systems Using Differentiation Method Based on Kharitonov's Theorem," IETE Journal of Research, vol. 68, no. 3, pp. 2079-2095, 2019.

APPENDIX

Parameters related to (2):

$$A = L_l^2 L_{f1} + 2L_l L_{f1} L_{f2} + L_{f2}^2 L_{f1}$$

$$B = L_{f2}^2 R_{f1} + 2R_{f1} L_l L_{f2} + 2R_{f2} L_{f1} L_{f2} + 2R_l L_{f1} L_{f2} + R_{f2} L_{f1} L_l + R_l L_{f1} L_l + L_l^2 R_{f1} + L_l L_{f1} L_{f2} + L_{f2}^2 R_c + 2L_{f2} L_l R_c + L_l^2 R_c + R_c L_{f1} L_{f2} + R_c L_{f1} L_l$$

$$C = 2L_{f2} R_{f1} R_{f2} + 2L_{f2} R_{f1} R_l + 2L_l R_{f1} R_{f2} + R_{f2}^2 L_{f1} + 2L_{f1} R_l R_{f2} + L_{f1} L_l R_l + R_l^2 L_{f1} + L_l R_l R_{f1} + L_{f2}^2 / C_f + 2L_{f2} L_l / C_f + L_l^2 / C_f + 2L_{f2} R_c R_{f2} + 2L_{f2} R_l R_c + 2L_l R_c R_{f2} + 2L_l R_l R_c + R_{f1} R_c L_{f2} + R_{f1} R_c L_l + L_{f1} L_{f2} / C_f + L_{f1} L_l / C_f + L_{f1} R_c R_{f2} + L_{f1} R_c R_l$$

$$H = R_{f1} L_{f2} + R_{f1} L_l / C_f + R_{f1} R_c R_{f2} + R_{f1} R_c R_l + L_{f1} R_{f2} + L_{f1} R_l / C_f + 2L_{f2} / C_f + 2L_{f2} R_l / C_f + 2R_{f2} L_l / C_f + 2L_l R_l / C_f + R_{f2}^2 R_c + 2R_{f2} R_l R_c + R_l^2 R_c - R_c^3 + R_{f2}^2 R_{f1} + 2R_{f2} R_{f1} R_l + R_{f1} R_l^2$$

$$F = R_{f1} R_{f2} + R_{f1} R_l / C_f - 3R_c^2 / C_f + R_{f2}^2 / C_f + 2R_{f2} R_l / C_f + R_l^2 / C_f$$

$$E = 3R_c / C_f^2$$

$$D^* = 1 / C_f^3$$

$$K = L_{f2}^2 R_c + R_c L_{f2} L_l + L_l L_{f2} R_c + L_l^2 R_c$$

$$L = L_{f2}^2 / C_f + L_{f2} L_l / C_f + L_{f2} L_l / C_f + L_l^2 / C_f + R_c L_{f2} R_{f2} + R_c L_{f2} R_l + R_c L_{f2} R_{f2} + R_c L_l R_{f2} + R_l L_{f2} R_c + R_l L_l R_c + R_c L_l R_{f2} + R_c L_l R_l + R_c^2 L_{f2} + R_c^2 L_l$$

$$O = L_{f2} R_{f2} / C_f + L_{f2} R_l / C_f + L_{f2} R_{f2} / C_f + R_{f2} L_l / C_f + L_{f2} R_l / C_f + L_l R_l / C_f + L_l R_{f2} / C_f + L_l R_l / C_f + R_c R_{f2}^2 + R_{f2} R_l R_c + R_{f2} R_l R_c + R_c R_l^2 + 2L_{f2} R_c / C_f + R_{f2} R_c^2 + R_l R_c^2 + 2R_c L_l / C_f$$

$$N = L_{f2} / C_f^2 + L_l / C_f^2 + 2R_{f2} R_c / C_f + 2R_l R_c / C_f + R_{f2}^2 / C_f + R_{f2} R_l / C_f + R_l R_{f2} / C_f + R_l^2 / C_f$$

$$M = R_{f2} / C_f^2 + R_l / C_f^2 .$$

Parameters related to (4):

$$Y = K_{i1} K_{i2} J - K_{i1} K_{i2} J w_g$$
$$Z = J^2 w_g$$
$$K = K_{i1} D J w_g .$$

Parameters related to (5):

$$a_6 = J^2 L_{f2}^2 R_c + R_c L_{f2} L_l + L_l L_{f2} R_c + L_l^2 R_c w_g + K_{i2} J L_l^2 L_{f1} + 2L_l L_{f1} L_{f2} + L_{f2}^2 L_{f1} K_{i1} - K_{i1} w_g$$

$$a_5 = J^2 L_{f2}^2 / C_f + L_{f2} L_l / C_f + L_{f2} L_l / C_f + L_l^2 / C_f + R_c L_{f2} R_{f2} + R_c L_{f2} R_l + R_c L_{f2} R_{f2} + R_c L_l R_{f2} + R_l L_{f2} R_c + R_l L_l R_c + R_c L_l R_{f2} + R_c L_l R_l + R_c^2 L_{f2} + R_c^2 L_l w_g + D J L_{f2}^2 R_c + R_c L_{f2} L_l + L_l L_{f2} R_c + L_l^2 R_c K_{i1} w_g + K_{i2} J L_{f2}^2 R_{f1} + 2R_{f1} L_l L_{f2} + 2R_{f2} L_{f1} L_{f2} + 2R_l L_{f1} L_{f2} + R_{f2} L_{f1} L_l + R_l L_{f1} L_l + L_l^2 R_{f1} + L_l L_{f1} L_{f2} + L_{f2}^2 R_c + 2L_{f2} L_l R_c + L_l^2 R_c + R_c L_{f1} L_{f2} + R_c L_{f1} L_l K_{i1} - K_{i1} w_g$$

$$a_4 = J^2 L_{f2} R_{f2} / C_f + L_{f2} R_l / C_f + L_{f2} R_{f2} / C_f + R_{f2} L_l / C_f + L_{f2} R_l / C_f + L_l R_l / C_f + L_l R_{f2} / C_f + L_l R_l / C_f + R_c R_{f2}^2 + R_{f2} R_l R_c + R_{f2} R_l R_c + R_c R_l^2 + 2L_{f2} R_c / C_f + R_{f2} R_c^2 + R_l R_c^2 + 2R_c L_l / C_f w_g + D J L_{f2}^2 / C_f + L_{f2} L_l / C_f + L_{f2} L_l / C_f + L_l^2 / C_f + R_c L_{f2} R_{f2} + R_c L_{f2} R_l + R_c L_{f2} R_{f2} + R_c L_l R_{f2} + R_l L_{f2} R_c + R_l L_l R_c + R_c L_l R_{f2} + R_c L_l R_l + R_c^2 L_{f2} + R_c^2 L_l K_{i1} w_g + K_{i2} J 2L_{f2} R_{f1} R_{f2} + 2L_{f2} R_{f1} R_l + 2L_l R_{f1} R_{f2} + R_{f2}^2 L_{f1} + 2L_{f1} R_l R_{f2} + L_{f1} L_l R_l + R_l^2 L f1 + L_l R_l R_{f1} + L_{f2}^2 / C_f + 2L_{f2} L_l / C_f + L_l^2 / C_f + 2L_{f2} R_c R_{f2} + 2L_{f2} R_l R_c + 2L_l R_c R_{f2} + 2L_l R_l R_c + R_{f1} R_c L_{f2} + R_{f1} R_c L_l + L_{f1} L_{f2} / C_f + L_{f1} L_l / C_f + L_{f1} R_c R_{f2} + L_{f1} R_c R_l K_{i1} - K_{i1} w_g$$

$$a_3 = J^2 L_{f2} / C_f^2 + L_l C_f^2 + 2R_{f2} R_c / C_f + 2R_l R_c / C_f + R_{f2}^2 / C_f + R_{f2} R_l / C_f + R_l R_{f2} / C_f + R_l^2 / C_f w_g + D J L_{f2} R_{f2} / C_f + L_{f2} R_l / C_f + L_{f2} R_{f2} / C_f + R_{f2} L_l / C_f + L_{f2} R_l / C_f + L_l R_l / C_f + L_l R_{f2} / C_f + L_l R_l / C_f + R_c R_{f2}^2 + R_{f2} R_l R_c + R_{f2} R_l R_c + R_c R_l^2 + 2L_{f2} R_c / C_f + R_{f2} R_c^2 + R_l R_c^2 + 2R_c L_l / C_f K_{i1} w_g + K_{i2} J R_{f1} L_{f2} + R_{f1} L_l / C_f + R_{f1} R_c R_{f2} + R_{f1} R_c R_l + L_{f1} R_{f2} + L_{f1} R_l / C_f + 2L_{f2} / C_f + 2L_{f2} R_l / C_f + 2R_{f2} L_l / C_f + 2L_l R_l / C_f + R_{f2}^2 R_c + 2R_{f2} R_l R_c + R_l^2 R_c - R_c^3 + R_{f2}^2 R_{f1} + 2R_{f2} R_{f1} R_l + R_{f1} R_l^2 K_{i1} - K_{i1} w_g$$

$$a_2 = J^2 R_{f2} / C_f^2 + R_l / C_f^2 w_g + D J L_{f2} / C_f^2 + L_l / C_f^2 + 2R_{f2} R_c / C_f + 2R_l R_c / C_f + R_{f2}^2 / C_f + R_{f2} R_l / C_f + R_l R_{f2} / C_f + R_l^2 / C_f K_{i1} w_g + K_{i2} J R_{f1} R_{f2} + R_{f1} R_l / C_f - 3R_c^2 / C_f + R_{f2}^2 / C_f + 2R_{f2} R_l / C_f + R_l^2 / C_f K_{i1} - K_{i1} w_g$$

$$a_1 = D J R_{f2} / C_f^2 + R_l / C_f^2 K_{i1} w_g + K_{i2} J 3R_c / C_f^2 K_{i1} - K_{i1} w_g$$

$$a_0 = -1 / C_f^3 .$$